

# ASSESSMENT OF NOISE BARRIER DIFFRACTION USING AN IN-SITU MEASUREMENT TECHNIQUE

G R Watts      TRL Limited, Old Wokingham Road, Crowthorne, Berkshire, RG45 6AU  
M Surgand      TRL Limited  
P A Morgan      TRL Limited

## 1. INTRODUCTION

Noise barriers are frequently employed in highway design to help mitigate the impact of traffic on roadside communities. The screening performance of barriers is dominated by sound that is diffracted over the top. In recent years there has been considerable interest in designing barrier profiles that are more efficient at improving screening performance over that provided by a simple thin screen. There is currently a requirement to characterise the performance of these devices so that designers can incorporate appropriate designs.

The European Standards group CEN TC 226/WG6 has developed draft standards on measuring in situ absorption and transmission loss of noise barriers [1]. There is currently interest in developing a method to quantify the diffraction efficiency of added devices. Such devices can take a variety of forms including multiple-edge profiles, absorptive T-shapes and cylinders. The present paper describes tests on such profiles using the Maximum Length Sequence (MLS) method to characterise acoustic performance. The main advantage of this technique is that measurements can be taken *in situ* in the presence of high extraneous noise e.g. at the edge of a busy motorway. Use was made of TRL's noise barrier test facility. This facility is situated on a flat grassland site, free of any reflecting surfaces which may affect recorded noise levels. At one end of the site a level section of asphalt has been laid to represent a typical road surface. A 20m long noise barrier is constructed adjacent to one edge of the asphalt. Using this set-up, measurements were taken on four different types of noise barrier including multiple edge, T-shaped and cylindrical designs.

## 2. THEORY

The basic geometry for characterising the diffraction efficiency of a noise barrier is shown in Figure 1. The microphone is not located in the deep shadow zone below the top of the barrier so ensuring that the diffracted component of the impulse response will be considerably greater in magnitude than any transmitted components. The diffracted component is extracted by means of an appropriate time window. Using a similar separation between source and receiver the measurement is repeated under free-field conditions. The ratio between the diffracted and free-field responses provides a measure of attenuation provided by the barrier profile.

The formula for calculating the insertion loss (the level difference with and without a barrier present) is given by

$$IL(f) = -10 \times \log_{10} \left\{ \frac{|H_b(f)|}{|H_i(f)|} \times \frac{d_b}{d_i} \right\}^2 \text{ dB}$$

where  $H_b(f)$  is the frequency response of the diffracted component impulse response,  $H_f(f)$  is the frequency response of the free-field impulse response and,  $d_b$  and  $d_f$  are the lengths of the shortest direct path through the barrier and the free-field path respectively.

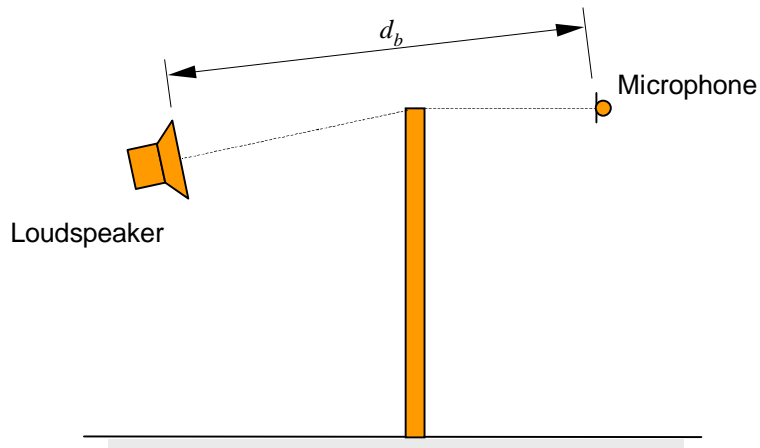


Figure 1: Test arrangement for characterising the diffraction efficiency of a noise barrier

### 3. MEASUREMENTS

#### 3.1 Profile Tested

The cross-sectional designs of the barriers tested are shown in Figure 2. For each barrier, the main upright was 2.0m high, 5.0m long and 0.12m thick and constructed from a 0.5 m high plane concrete plinth supporting from three panels held in place by I-section steel vertical beams. The panels were an aluminium box construction of dimensions  $2.5 \times 0.5 \times 0.12$  m. All surfaces on these panels were acoustically reflective.

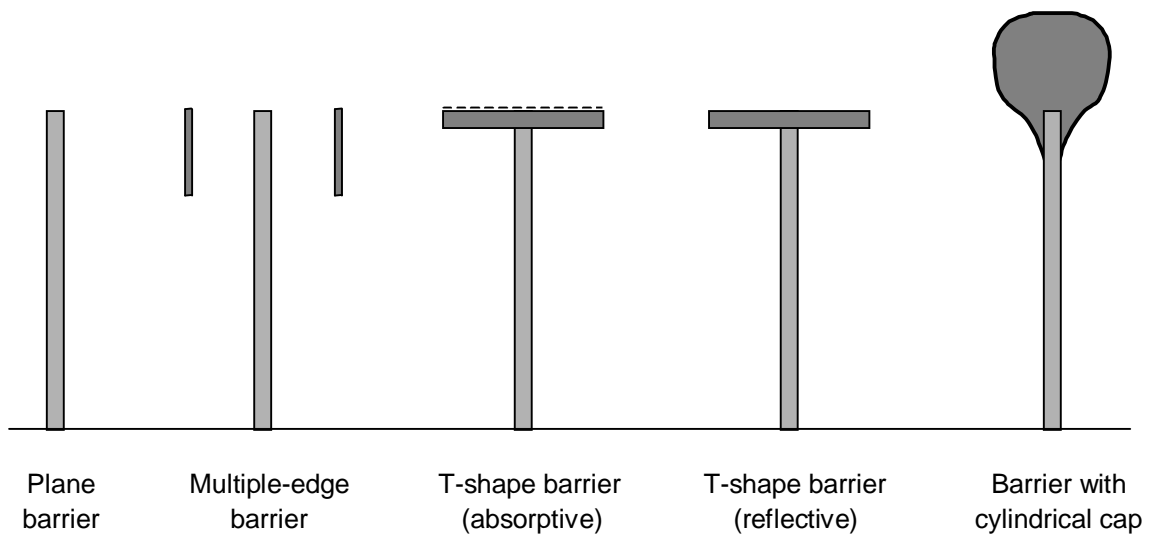


Figure 2: Noise barrier profiles tested on the barrier facility

For the T-shaped barriers the cross-piece was formed from two of the aluminium box-section panels, positioned perpendicularly to the plane section using a lightweight aluminium support frame attached to the main posts such that the overall height of the plane barrier was not increased. The panels used featured a sound absorptive face on one side and a reflective face on the other. The absorptive face was constructed from a perforated facing and a rockwool fill material. This resulted in this side of the panel having a mean absorption coefficient (0.25 – 5.0 kHz) of  $\alpha > 0.8$ . The other side of the panel was constructed from aluminium sheet without perforations and was therefore highly reflective. To create the absorptive T-shape profile shown in Figure 2, the absorptive face was placed uppermost while in the case of the reflective T-shape the panels were turned so that the reflective face was uppermost.

The multiple-edge barrier consisted of two additional side panels attached parallel to the main upright, one on either side (separation = 0.5 m), using a light structural steel beam to produce a design symmetrical about the vertical axis. The panels, constructed from thin sheet steel, were 0.5 m high and positioned with the upper edge flush with the top of the main barrier.

The cylindrical cap fitted to the plane barrier was manufactured by a Japanese engineering company, and consisted of a curved, hollow profile. The outer surface the profile was a perforated polycarbonate-sheet that enveloped a 50mm thick layer of mineral wool protected by a water and UV proof film.

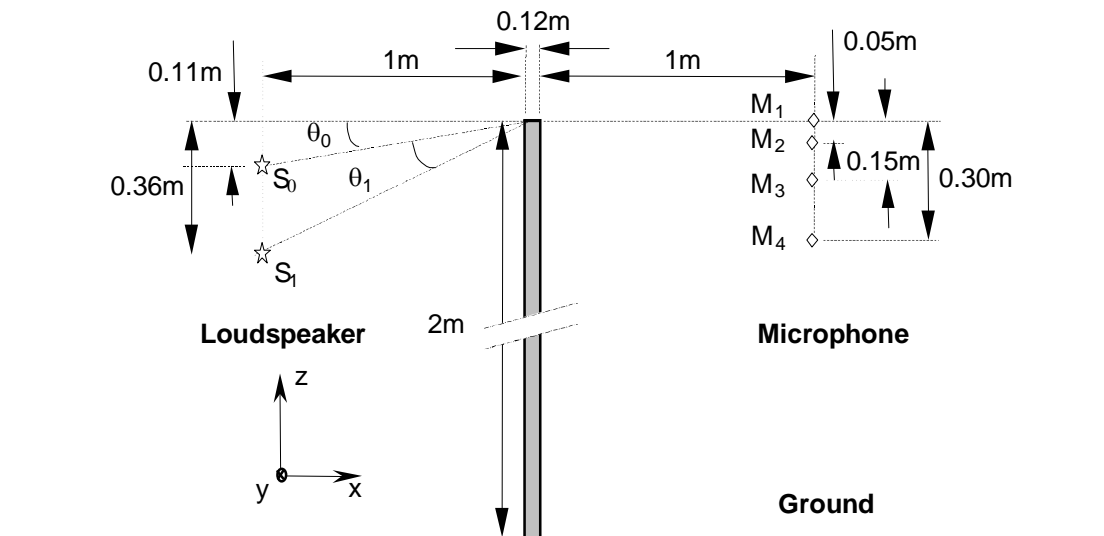
### 3.2 Measurement Method

A loudspeaker source and microphone were placed on opposite sides of the barriers and set at different heights for different inclinations in the vertical plane. The loudspeaker used was a 20 Watt speaker with the tweeter disabled so as to obtain a single source of sound. The microphone was a ½ inch condenser microphone. All measurements were performed with the loudspeaker and receiver microphone axis perpendicular to the top edge of the barrier (normal incidence in the horizontal plane). Two source positions and four microphone positions were used for each barrier configuration, resulting in 8 measurement combinations for each barrier, as shown in Figures 3 and 4. In all cases the same source and receiver heights were applied relative to the nearest diffracting edge, resulting in the same angles of inclination and these are summarised in Table 1.

	Identifier	Vertical position (below top of barrier) (m)	Inclination $\theta$ (°)
Source position	S <sub>0</sub>	0.11	6.3
	S <sub>1</sub>	0.36	19.8
Receiver position	M <sub>1</sub>	0.00	0.0
	M <sub>2</sub>	0.05	2.9
	M <sub>3</sub>	0.15	8.5
	M <sub>4</sub>	0.30	16.7

Table 1: Source and receiver heights used for measurements on Noise Barrier Test Facility

(a) Plane barrier



(b) T-shape

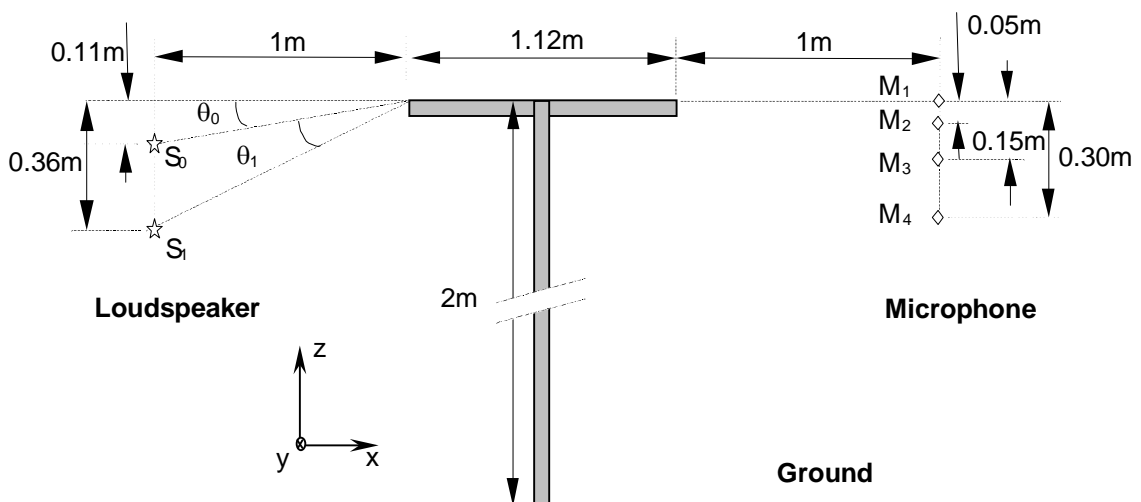
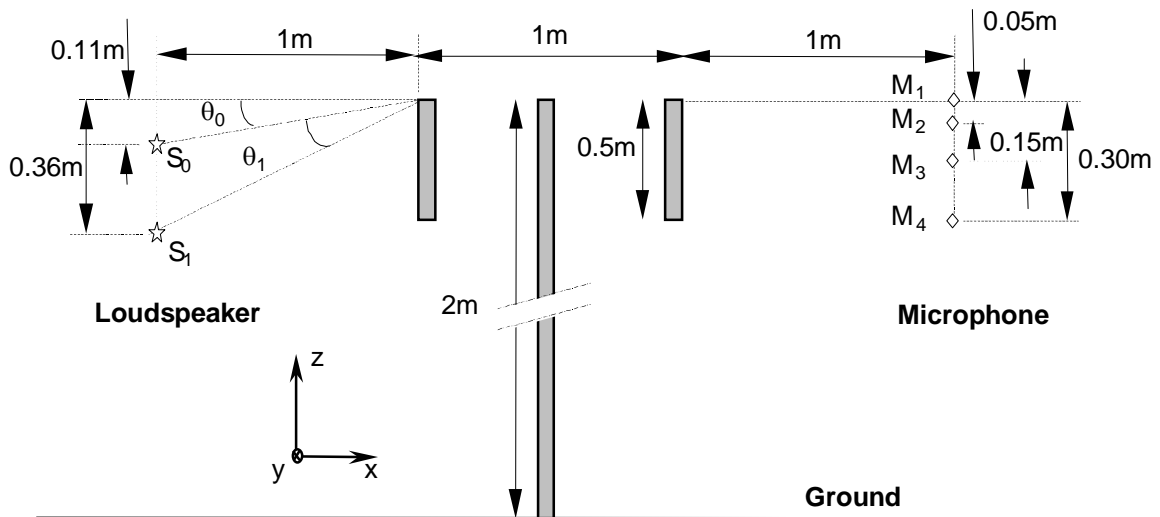


Figure 3: Position of source and microphone for plane and T-shaped barriers

(a) Multiple-edge



(b) Cylinder

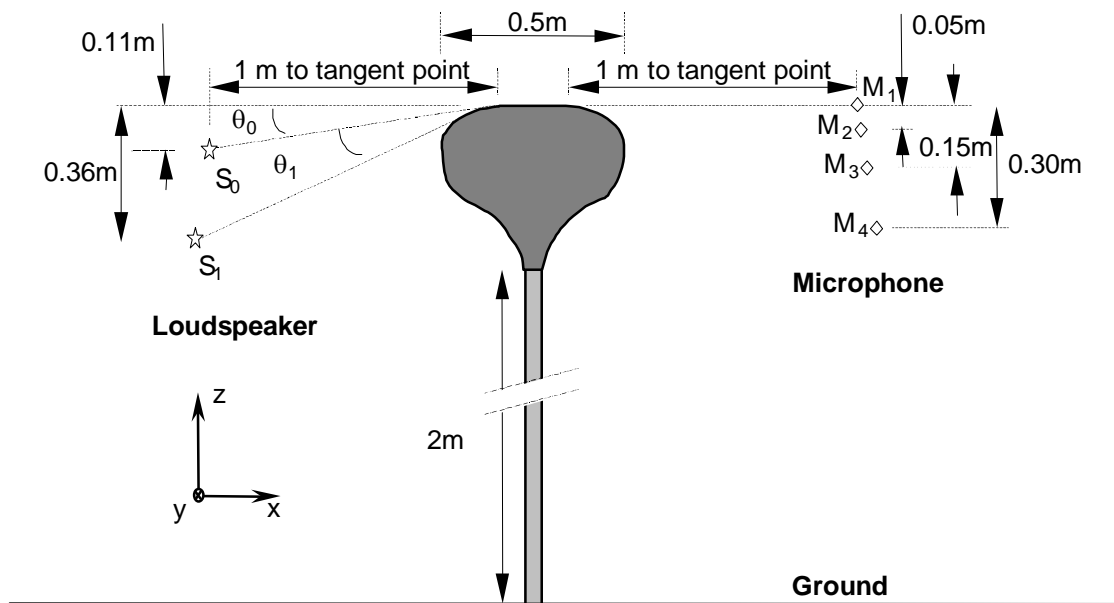


Figure 4: Positions of source and microphone for multiple-edge and cylindrical barriers

The horizontal separation between the barrier and these source/receiver positions was set at 1.0 m from the position of the leading/trailing diffracting edges respectively. This resulted in a vertical array of sources and receivers for the plane screen, the T-shape and multiple-edge barriers.

However, for the barrier with the cylindrical cap, the position of the diffracting edge was defined as the tangent point for the line of sight from any source or receiver position (Figure 4). Consequently, lower sources and receivers were further from the barrier centre unlike the case for the other options. The orientation of the sources corresponded to the angles which would be defined by a 3m tall barrier were the sources to be located in the middle of the nearside and farside carriageways of a motorway ( $S_1$  and  $S_0$  respectively). The orientation of the receiver positions corresponded to angles which would be defined by a standing adult at distances of 30, 10 and 5m from the 3m tall barrier. The receiver horizontal with the barrier top would of course be at a large distance from the barrier. For each individual measurement combination, the analysis software (MLSSA) was configured to use 16 averages. To reduce the disruptive influence of wind on the measurements, it was necessary to introduce a filter into the measurement set-up to filter out frequencies below 22.4 Hz. Without the filter the measurements took longer to make because many samples were flagged as invalid by the acquisition software. This may have resulted from the high spurious low frequency components produced by the turbulent airstream around the microphone. This filter was applied at the microphone amplifier by enabling the appropriate high-pass filter.

It was known that wind can have a deleterious effect on the performance of a barriers in the far-field due to turbulent scattering of sound waves into the shadow zone of the barrier and by refraction caused by wind speed gradients. However, it was not known if this would affect results close to the barrier edge. To take account of this possible affect an anemometer (Wind-tracker) was used in order to keep a record of the wind speed and direction over the duration of the measurements. The component of the wind vector perpendicular to the plane of the barrier was averaged over the period of each measurement. In general, for each set-up geometry, 4 repeat measurements were taken with a positive wind and 4 measurements were taken with a negative wind component. This was achieved by carrying out a set of measurements for each geometry and then swapping the positions of microphone and loudspeaker and repeating the measurements. With a total of 8 repeat measurements and corresponding positive and negative wind components it was possible using linear regression to obtain a good estimate of the insertion loss at zero wind speed.

## **4. RESULTS**

### **4.1 Comparison Of Barrier Profiles Using MLS**

The insertion losses normalised to zero wind speed were plotted against frequency for each option tested. Figure 5a and Figure 5b show the results for 2 measurement positions (microphone level with the barrier top and source at 11 cm and 36 cm below the top). The results indicate the main tendencies shown in the full set of results that have been analysed for all 8 measurement geometries, (i.e. 2 source positions and 4 microphone positions).

Generally for all options there is a rise of insertion loss with increasing frequency. At the lowest frequency the insertion losses are comparable, but diverge as the frequency increases. At most frequencies the absorptive T-shape produces the greatest insertion loss and the cylinder and plane barrier the least. The largest differences are close to 15 dB(A). At the three lowest frequencies the trident profile produced the largest insertion loss while at 850Hz and above the absorptive T-shape produced the largest effect. The performance of the reflective T-shape option tends to be intermediate lying between that of the trident and that of the plane and cylinder options.

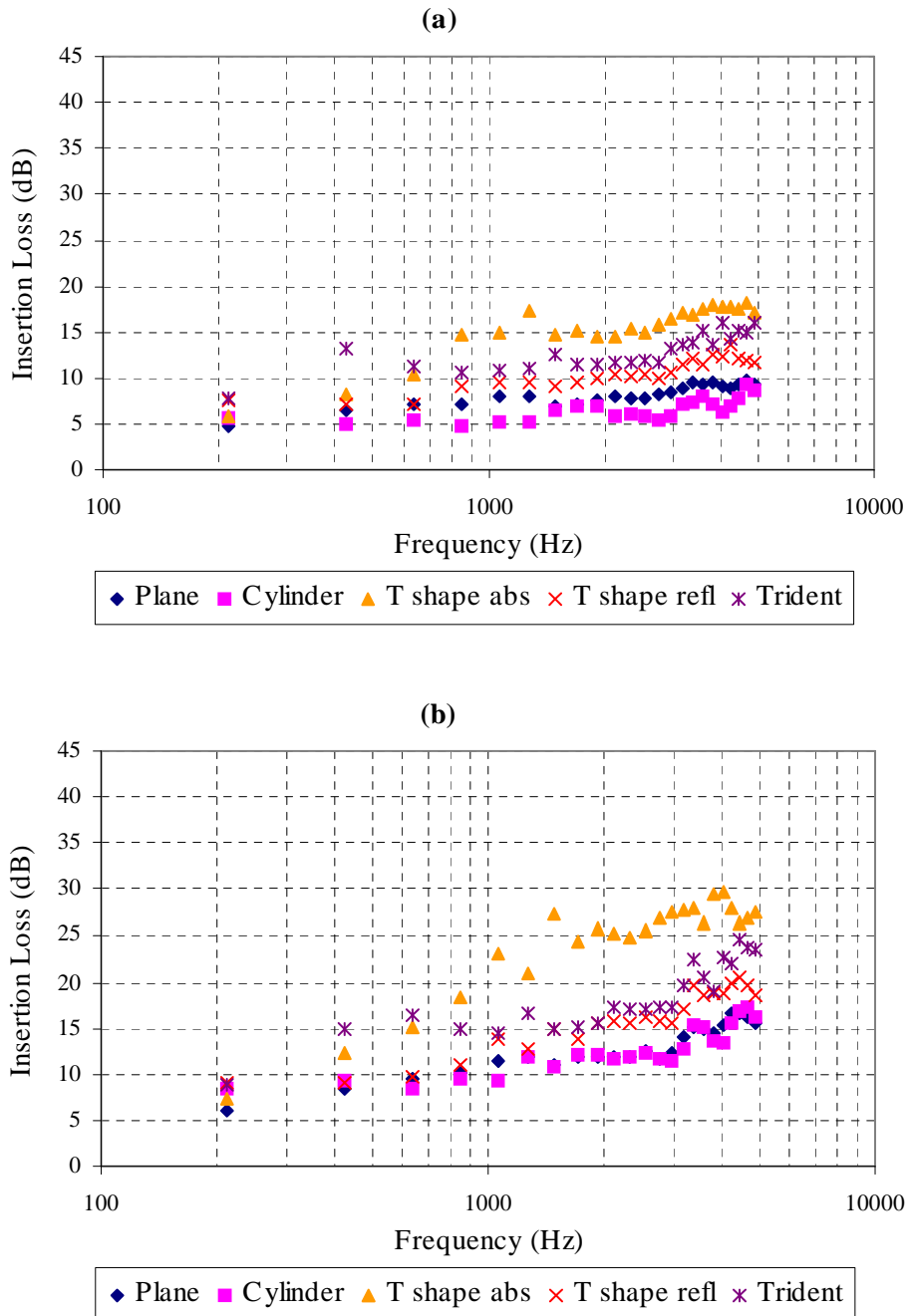


Figure 5: Insertion loss spectrum for receiver level with profile top (a) for source at 11 cm below top and (b) for source at 36 cm below top

In order to gain an insight into the performance of the barriers with typical traffic noise, a single number rating of diffraction efficiency was calculated based on a standard traffic noise spectrum given in EN 1793-3 [2]. This weights the insertion losses at a number of measured frequencies by corrections based on the third-octave A-weighted spectrum. Since the frequencies at which the

insertion losses were measured were based on window length they were not at third octave centre frequencies and it was decided to select the insertion losses closest to each third octave band frequency. If  $IL_i$  is the insertion loss at the  $i$ th frequency and  $L_i$  is the normalised A-weighted sound pressure level of traffic noise in the nearest third-octave frequency band, then the single number rating of diffraction efficiency SNRD is given by:

$$SNRD = -10 \text{Log} \left[ \frac{\sum_i 10^{\frac{L_i}{10}} \cdot 10^{\frac{-IL_i}{10}}}{\sum_i 10^{\frac{L_i}{10}}} \right]$$

The summation is over 12 third octave band frequencies corresponding to most of the frequency bands from 200 to 5000Hz. Since the measured frequency intervals was 212Hz (corresponding to an effective window length of 4.7ms), at low frequencies the spacing was too broad to include all one-third octave bands. Consequently the measured levels corresponding to the centre frequencies of 250, 316 and 500Hz are missing from the above calculation. Table 2 lists the SNRDs for the 5 options tested for all the test arrangements.

Geometry (Speaker / microphone position)	Single number rating of Insertion Loss				
	Plane	Trident	Absorptive T-shape	Reflective T- shape	Cylinder
11/0	7.5	11.3	13.2	9.2	5.6
11/05	8.3	12.1	13.9	13.3	6.7
11/15	9.6	14.0	15.2	12.1	8.5
11/30	11.5	16.3	16.4	13.8	10.6
36/0	10.9	15.3	17.8	12.4	10.4
36/05	11.5	16.2	16.1	12.9	11.2
36/15	12.6	17.8	17.0	14.8	12.9
36/30	14.2	19.9	17.3	16.0	15.5
Average:	10.8	15.4	15.9	13.1	10.2

Table 2: Single number ratings by barrier option

It can be seen that the order of overall performance reflects the trends noted in the insertion loss spectra i.e. the absorptive T-shape and trident options showing relatively good performance but the cylindrical and plane barriers having similar relatively poor performance. The reflective T-shape shows an intermediate performance.

## 5. DISCUSSION

The MLS based technique using signal separation proved reliable and robust in most cases. During initial tests under windy conditions many samples were flagged as invalid by the MLSSA signal processing system. This was considered to be due to the lack of coherence between the input signal to the speaker and the output signal from the microphone that were cross-correlated during analysis to obtain the impulse response. By inserting a 22.4Hz high pass filter in microphone amplifier this problem was significantly reduced. It is likely that the turbulence around the microphone created under windy conditions was producing high levels of low frequency noise that may have caused distortion of the microphone signal.

It was possible to use a relatively small, low output loudspeaker (20 W) during the current trials although under high levels of ambient noise e.g. at the roadside, it may be necessary to consider a more powerful source. However such a source should remain compact otherwise the geometry from source to diffracting edge is not well defined, as contributions can arise from the edges of the loudspeaker cone which may present a significantly different angle of incidence than that defined by the loudspeaker axis. The geometry that was developed for these tests was based on a consideration of typical source and receiver positions in front of and behind a barrier positioned close to a typical motorway. However due to time constraints, only a single angle of incidence in the horizontal plane was used i.e. zero incidence. Since a traffic stream can be considered as an infinite line source, to fully characterise the performance of a barrier screening traffic noise it is necessary to consider other angles of incidence. It is therefore recommended that for further work, measurements should not be restricted to normal incidence.

The results of this study have established that the MLS technique is clearly sensitive enough to demonstrate differences between barrier profiles. Compared with a simple plane barrier, differences of up to approximately 15 dB were found. As expected the use of an absorptive material on the upper surface of the T-shaped profile improved the insertion loss considerably. From Table 2, the single number rating of insertion loss for the absorptive T shape was over 2.5 dB(A) greater than for the reflective T-shape. This is thought to be due to the action of the absorber extracting energy from the waves propagating over this surface. Similar improvements compared with the plane barrier were produced by the multiple-edge design. This works on a different principle from the absorptive T-shape profile since no absorptive material is involved. The two side panels of the multiple-edge profile act as further diffracting edges that scatter sound waves advancing over the surface of the device leaving less sound energy to be diffracted into the shadow zone. The device appears to be particularly effective over the range 400-800 Hz. This suggests an additional mechanism may be involved. Due to internal reflections standing waves could be set up between these side panels and the main barrier. Since the separation is 0.5 m, a half wave of wavelength 1 m could be excited or a full wave of wavelength 0.5 m. The corresponding frequencies would be 340 and 680 Hz respectively. Such standing waves would reduce the contribution eventually diffracted into the shadow zone, thereby improving the insertion loss in frequency bands centred on these particular frequencies.

The absorptive cylinder had little effect when compared with a plane barrier. It is possible that the absorptive material had degraded over time (the cylinder sections were over 7 years old) and therefore was not fully effective. Theory shows that a rounded edge is more effective in diffracting sound into the shadow zone than is the classic "knife edge". If the absorptive material had been significantly degraded there would be no improvement in screening performance.

From a practical point of view it is performance in the far field that is generally of greater importance and therefore in any extension of the work the results of measurements made close to the barrier should be compared with results at greater distances [3]. In this way the most appropriate measurement set up for MLS measurements can be determined.

## 6. CONCLUSIONS

An MLS based analysis technique has been demonstrated to be a reliable and robust method for characterising the diffraction efficiency of noise barriers. The results of this study have established that the technique is sensitive enough to demonstrate differences between barrier profiles. Depending upon the barrier type, the current apparatus may require upgrading with a more powerful loudspeaker to improve the signal-to-noise ratio. This may be particularly important when noise from adjacent traffic is high. The absorptive T-shape and multiple-edge profiles were observed to offer the greatest improvement in screening performance over the plane screen. Further measurements are required to look at the effects on screening performance at angles of incidence other than normal incidence. The effects of wind on performance could also be examined by taking further measurements under a greater range of wind speeds.

## 7. REFERENCES

- [1] **European Committee for Standardisation (2000)**. Pr ENV 1793-5. Road traffic noise reducing devices – Test method for determining the acoustic performance – Part 5: Intrinsic characteristics – In-situ values of sound reflection and airborne sound insulation. Brussels, Belgium: CEN.
- [2] **European Committee for Standardisation (1998)**. Pr ENV 1793-3. Road traffic noise reducing devices – Test method for determining the acoustic performance – Part 3: Intrinsic characteristics – Standardised traffic noise spectrum. Brussels, Belgium: CEN.
- [3] **Watts G R, D H Crombie and D C Hothersall (1994)**. Acoustic performance of new designs of traffic noise barriers: Full scale tests. *Journal of Sound and Vibration* 177 (3), 289-305.